THE JOURNAL OF PHYSICAL CHEMISTRY B

Article

pubs.acs.org/JPCB

Effects of Organic Solvent and Crystal Water on γ-Chymotrypsin in Acetonitrile Media: Observations from Molecular Dynamics Simulation and DFT Calculation

Lijuan Zhu, Wei Yang, Yan Yan Meng, Xiuchan Xiao, Yanzhi Guo, Xuemei Pu,* and Menglong Li*

Faculty of Chemistry, Sichuan University, Chengdu 610064, People's Republic of China

ABSTRACT: The use of enzymes in nonaqueous solvent has been one of the most exciting facets of enzymology in recent times; however, the mechanism of how organic solvent and essential water influence on structure and function of enzyme has been not satisfactorily explained in experiments, which limit its further application. Herein, we used molecular dynamics (MD) simulation to study γ-chymotrypsin in two types of media (viz., acetonitrile media with inclusion of 151 crystal water molecules and aqueous solution). On the basis of the MD result, the truncated active site modes containing two specific solvent molecules are furthered studied at the B3LYP/6-31+G(d,p) level of theory within the framework of PCM model. The results show that the acetontrile solvent gives rise to an extent deviation of enzyme structure from the native one, a drop in the flexibility and the total SASA of enzyme. The QM study further reveals that the structure variation of the active pocket caused by acetonitrile would lead to a weakened strength in the catalytic H-bond network, a drop in the pK_a value of His57, and an increase in the proton transfer barriers from the Ser195 to the His57 residue, which may contribute to the drop in the enzymatic activity in acetontrile media. In addition, the crystal waters play an importance role in retaining the catalytic H-bond network and weakening the acetonitrile-induced variations above, which may be associated with the fact that the enzyme could retain catalytic activity in microhydration acetonitrile media.

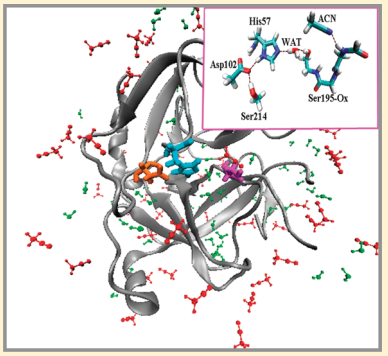

1. INTRODUCTION

The use of enzymes in nonaqueous media has been one of the most exciting facets of enzymology in recent times, since it has higher selectivity and thermostability and lower side reactions in the media than that in aqueous environment, thus provide numerous synthetic and processing advantages.[1−5] However, native enzymes universally exhibit very low activities in organic solvents, often 4 or 5 orders of magnitude lower than in aqueous solutions. It is not surprising because enzymes have evolved naturally to function in predominantly aqueous environments. The reduced activity in organic solvent limits its application in industry. Thus, many efforts from experiments are devoted to shedding light on the influence of the organic solvent and the role of water on enzyme structure and function.

It has been recognized that to retain their activity in anhydrous solvents, proteins still require some water molecules (viz., essential water) to be presented. The control of water is exerted by the number of molecules bound to the enzyme rather than its level in the organic solvent. Some researches have reported that the organic solvent drop the activity of an enzyme through stripping off water molecules bound to the enzyme,[3,5,6] and the essential water would increase the flexibility of the enzyme in nonaqueous media, accordingly favoring the activity of enzyme.[7,8] However, some investigations have indicated that there are no direct correlations of the enzymatic activity with its flexibility,[5,9] and the organic solvent penetration into the active site of enzymes should be one of the main reasons, since it would induce variation in the conformation of the active site.[2,10] These observations above have showed that factors that contribute to this activity drop are complicated. In fact, it is difficult for experiment to probe atomistic details of organic solvent−enzyme−essential water interaction and determine subtle changes in the active site because of the complexity of the enzyme structure and the molecular nature of the issue. Therefore, the molecular mechanism of solvent effects on the enzymatic activity has been disputed.

Molecular dynamics simulations could provide a molecular level view of the solute−solvent interaction and can reveal dynamic behavior of proteins. Thus, the method has been widely used to study enzymes in aqueous solution[11−14] and nonaqueous media[3,15−21] to obtain microscopic information at the molecular level and supplement experimental investigations. Toba[15] investigated the structure of γ-chymotrypsin in hexane media. Soares[16] used the MD method to discuss the effects of several hydration conditions on structure variations of two model proteins (ubiquitin and cutinase) and the enantioselectivity of cuitase[17] in hexane. Piñeiro performed a molecular dynamics study of triosephosphate isomerase in water/decane mixtures[18] and discussed mainly the structure and dynamics of the enzyme as well as the mobility of the solvent. Micaelo[19] comparatively studied the hydration mechanism of serine

Received: August 27, 2011
Revised: February 8, 2012
Published: February 9, 2012

protease in five organic solvents with different polarities using the MD method. Nemat-Gorgani[20] used the MD method to study conformational changes of α-chymotrypsin in a TFE/water mixture. The conformation stability of lipase B in six solvents was investigated by Feng.[21]

On the whole, theoretical studies on enzymes in nonaqueous media are still limited, and only a few MD studies in the literature are found. These MD observations provide useful molecular information for understanding correlations among the solvent polarity, the structure of the enzyme, the flexibility, and the hydration of enzyme from the viewpoint of dynamics behavior. However, it is noted that these studies lacked quantum mechanics (QM) calculation. As known, the QM method could describe the chemical reaction involving the breaking and formation of bonds and well characterize intermolecular interaction at the electronic level, which could not be accessible for the semiempirical MD method. Thus, the information derived from a QM study could provide new insight into the structure and function of an enzyme in organic media and could importantly contribute to the refinement of molecular mechanism on the regard. On the basis of these considerations above, we herein combined MD and QM methods to present a comprehensive theoretical study on chymotrypsin in acetonitrile media.

Chymotrypsin is a member of the diverse group of enzymes known as serine protease and one of the most used enzymes in the catalysis of peptide bond synthesis.[22,23] Furthermore, it has been used for peptide and amino acid ester syntheses in different nonaqueous media.[24−28] Its catalytic mechanism depends on three amino acid residues (viz., histidine 57, aspartate 102, and serine 195), which form a hydrogen bond network (see Figure 1). By means of the network, the catalytic

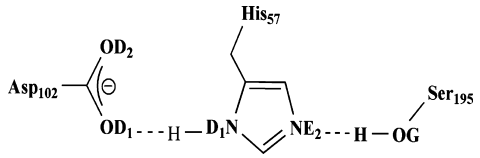

Figure 1. The catalytic triad of serine protease. Symbols of oxygen and nitrogen atoms are derived from the PDB file of the enzyme. The dotted lines denote H-bonds.

reaction is performed.[22,29] Acetonitrile was chosen in the work since it was one of the most common organic media for nonaqueous enzymatic catalysis[24,30] and has not been studied in previous MD simulations on chymotrypsin. Thus, the work will focus on chymotrypsin in acetonitrile media with inclusion of crystal waters. As a reference, the enzyme in aqueous solution was also studied using the MD and QM methods. Our objective is to provide systematic information from the dynamics behavior (viz., MD result) and QM calculation for better understanding the effect of polar organic solvent on the structure and function of the enzyme by comparison of the two systems. In addition, we also wish to gain insight into the role of the crystal waters in modulating the organic solvent effects, which are helped to understand the role of essential water in enzymatic structure and reactivity in nonaqueous media.

2. COMPUTATIONAL DETAILS

2.1. MD Simulation. Molecular dynamics (MD) simulations were performed using the program AMBER 10.0.[31] The AMBER03 force field[32] was used for γ-chymotrypsin, and water was represented by the TIP3P model.[33] The GAFF[34] force field was utilized for acetonitrile, and the atom type of the acetonitrile molecule was allocated using the AMTECHAMBER module.[35]

The starting coordinate of native crystallized γ-chymotrypsin was obtained from the Brookhaven Protein Data Bank (the PDB entry code is 2GCH[36]), which contains 151 crystal waters. In the X-ray structure, the protein molecule consists of three peptide segments (1−11, 16−146, 151−246) connected by disulfide bonds. So it was only 237 residues that were used in the MD simulation. Three chloride ions were introduced near positively charged groups as counterions to neutralize the protein charge using columbic potential terms. In aqueous and acetonitrile solutions, we retained all crystal waters (151). Extra water molecules and acetronitrile molecules were added using the XLEAP utility. The rectangle periodic box was set up so that any solute atom is at least 12 Å from any box edges for the acetonitrile system, but 10 Å for the aqueous system. As a result, the acetonitrile system includes 151 resolved water molecules and 2625 acetronitrile molecules (labeled as ACN). The aqueous system contains 10 454 water molecules (labeled as WAT).

To remove bad contacts in the initial geometries of the two systems, three energy minimizations (5000 steps for the solvent molecules followed by 5000 steps for the protein and, finally, 5000 steps for the whole system) were done by the same procedure: the steepest descent method for the first 3000 steps for relaxation of the close contacts, followed by conjugate gradient algorithm for the remaining part. After minimizations, the systems are heated gradually from 0 to 300 K within 120 ps. Following that, 2 ns dynamics simulations were carried out with periodic boundary conditions in the NVT ensemble at 300 K using the Berendsen temperature coupling.[37] Finally, 6 ns NPT simulation (T = 300 K and P = 1 atm) was performed in the canonical ensemble. A time step of 1 fs was utilized for all MD simulations. The SHAKE algorithm[38] was applied to constrain all the bonds involving a hydrogen atom with a tolerance of 1.0×10^{-5} Å. Nonbond interactions were handled with a 12 Å atom-based cutoff. The particle-mesh-Ewald (PME) method[39,40] was applied to treat the long-range electrostatic interactions. The last 1 ns trajectory was saved every 1 ps for analysis. All of the MD results were analyzed using the analysis module of AMBER 10.0 and some other developed specific trajectory analysis software.

2.2. QM Calculation. QM calculations involve only the reactive site, which consists of five truncated residues and two solvent molecules (a detail description is provided later). The truncated active site models were optimized at the B3LYP/6-31+G** level of theory, which has been proven to successfully reproduce geometries and energies of hydrogen bonds for some enzymes.[41,42] To include the dielectric effects from the solvent and the protein surrounding, polarizable continuum models (PCM)[43] were used in all optimizations unless otherwise stated. The Cα atoms were kept fixed during the optimization to consider the protein environment, which was excluded in the active site model system. All minima and transition states were verified by vibrational frequency analysis at the same level of theory. Natural bond orbital (NBO) analysis introduced by Weinhold and co-workers[44] was carried out to discuss orbital interactions for all the optimized geometries at the same level of theory using NBO program incorporated in Gaussian 09. Nuclear shielding constants of H atoms involving intermolecular H-bonds were calculated using the gauge-independent

dx.doi.org/10.1021/jp3002405 | J. Phys. Chem. B 2012, 116, 3292−3304

atomic orbital (GIAO) method.[45,46] The ^{1}H chemical shift is the difference of isotropic shielding constants of the studied system with respect to the tetramethylsilane (TMS) reference molecule. To be comparable, the calculation of the nuclear shielding of the reference compound and the studied systems were carried out at the same level of theory.

The p*K*a value of His57 was calculated by means of a method[47,48] in which the acid dissociation process was represented as a thermodynamics cycle, as showed in the following:

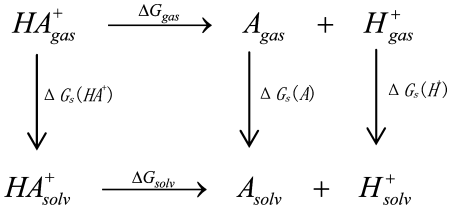

In this cycle, ΔG_{gas} and ΔG_{solv} denoted the free energy of deprotonation in the gas and solution, respectively. $\Delta G_s(X)$ represents the free energy of solvation of species X. The p*K*a was obtained in terms of equations as following:

$$pK_a = -\log K_a \quad (1)$$

$$\Delta G_{solv} = -2.303RT \log K_a \quad (2)$$

$$pK_a = \frac{\Delta G_{solv}}{2.303RT} \quad (3)$$

where

$$\Delta G_{solv} = \Delta G_{gas} + \Delta\Delta G_s \quad (4)$$

$$\Delta G_{gas} = \Delta G_{gas}(A) + \Delta G_{gas}(H^+) - \Delta G_{gas}(HA^+) \quad (5)$$

$$\Delta\Delta G_s = \Delta G_s(A) + \Delta G_s(H^+) - \Delta G_s(HA^+) \quad (6)$$

The PCM models were introduced in the NBO and GIAO calculations. All quantum mechanics calculations were performed with the program Gaussian 09.[49]

3. RESULTS AND DISCUSSIONS

3.1. MD Simulation. *3.1.1. Structure of Protein.* In the part, root-mean-square deviation (RMSD) and root-mean-square fluctuation (RMSF) as well as radius of gyration are calculated and served as indicators to describe solvent effects on the overall structure of the γ-chymotrypsin. The RMSD is for the deviation from the crystal structure of the protein in aqueous solution, and the RMSF values are calculated in comparison with the average coordinates of the trajectory. The RMSD values of total protein in the two media are plotted as a function of time in Figure 2. The calculated RMSD and RMSF values of the last 1 ns trajectories are listed in Table 1.

As shown in Table 1, the ACN system has higher RMSD's compared with WAT, indicating that the structure of the protein in the acetonitrile media has a larger deviation from the starting crystal structure. Similar observations were found in previous research.[15,19,50,51] The RMSF about the averaged equilibrium conformation is often served as an indicator to estimate flexibility of the protein, which is also considered to be a character related to the protein activity.[21,52] Data in Table 1 show that the RMSF of all atoms and backbone atoms of the proteins in the two systems follows the order of ACN < WAT.

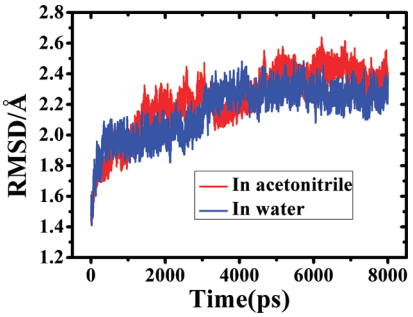

Figure 2. The RMSD values of all atoms of γ-chymotrypsin with respect to the simulation time in aqueous solution (labeled as WAT) and acetonitrile media (labeled as ACN). The RMSD is for the deviation from the crystal structure of γ-chymotrypsin in aqueous solution.

It suggests that the organic solvent decreases the flexibility of the protein, which may be partly associated with the drop in activity in organic media. Herein, we also were concerned with the variation in the active site. In aqueous and acetonitrile media, the active site residues (see Table 1) show much lower RMSD and RMSF values than the protein's average. MD simulations on γ-chymotrypsin in hexane[15] and acyl-chymotrypsin in aqueous solution[53] also found that the active site residues have smaller fluctuations than the rest of the protein. The relative rigidity of the catalytic residues in both polar and nonpolar medium should contribute to the experimental observation that the protein still retains catalytic activity in an organic solvent with a low water content.[54−57]

The radius of gyration is defined as the mass-weighted rms distance of a collection of atoms from their common center of mass.[58] Hence, this analysis gives us insight into the overall dimensions of the protein. The results of the gyration calculation performed over the last 1 ns simulations are collected in Table 2. The values are equal (16.66) in the ACN and WAT systems, indicating that the protein remains globular, and no unwinding or denaturation is observed within the simulation time.

3.1.2. SASA (Solvent-Accessible Surface Area) and Thermostability of Protein. Solvent accessible surface area (SASA) can be considered to be an indicator of how different parts of a protein can be affected by media. The SASA is calculated using the program VMD,[59] defined by rolling a probe of given size (1.4 Å) around a van der Waals surface of the protein. Table 2 gives the SASA values calculated over the last 1 ns simulation. As shown in Table 2, the total SASA in acetonitrile media is smaller than that in aqueous solution. To gain more insight into the variation of SASA, we analyzed SASA variations of hydrophobic and hydrophilic residues. The percentage of hydrophilic SASA[30] and hydrophobic SASA[60,61] relative to the total SASA (SASA %) are calculated in the two media and listed in Table 2. The percentage of SASA (hydrophobic %) in the ACN system is higher than that in WAT, and the percentage of hydrophilic (hydrophilic %) shows the opposite trend. The observation indicates that both the hydrophobic and hydrophilic side chains reorient themselves on the protein surface in acetonitrile media. Thereby, they experience a decrease and increase in SASA with a variation of in the solvent composition. For example, the hydrophobic residues in the acetonitrile media become more exposed to the organic solvent, and the hydrophilic residues become more

dx.doi.org/10.1021/jp3002405 | J. Phys. Chem. B 2012, 116, 3292−3304

Table 1. RMSD, RMSF Values and Their Standard Deviation for the Active Site Residues and the Protein over Last 1 ns Trajectories (Å)[a]

	WAT[b]		ACN[c]	
system	RMSD	RMSF	RMSD	RMSF
His57	0.261 ± 0.051	0.167 ± 0.044	0.250 ± 0.052	0.167 ± 0.049
Asp102	0.172 ± 0.042	0.133 ± 0.035	0.201 ± 0.055	0.136 ± 0.044
Ser195	0.382 ± 0.121	0.254 ± 0.087	0.385 ± 0.197	0.305 ± 0.218
total	2.255 ± 0.057	1.000 ± 0.064	2.381 ± 0.057	0.915 ± 0.060
backbone	1.463 ± 0.070	0.646 ± 0.055	1.569 ± 0.061	0.574 ± 0.053

[a]The RMSD and RMSF values are for deviations from the crystal structure of γ-chymotrypsin in aqueous solution and the average structure of γ-chymotrypsin over the last 1 ns equilibrium trajectory, respectively. [b]WAT denotes the γ-chymotrypsion in aqueous solution. [c]ACN denotes the γ-chymotrypsion in acetonitrile media with inclusion of 151 crystal waters.

Table 2. Summary of Gyration Radius, Total SASA, Hydrophobic and Hydrophilic SASA, Average Numbers of Solvent Molecules Residing in the Active Pocket, Average Number of Intraprotein Hydrogen Bonds (HB), Average Number of Salt Bridges (SB), and Standard Deviations over Last 1 ns Simulation for the γ-Chymotrypsin in Aqueous Solution (WAT) and Acetonitrile Media (ACN)

system	WAT	ACN
gyration radius (Å)	16.66 ± 0.03	16.66 ± 0.04
	SASA	
SASA (× 10^3 Å^2)	11.62 ± 0.11	11.101 ± 0.09
hydrophobic %	27.60 ± 0.51	28.31 ± 0.53
hydrophilic %	72.40 ± 0.91	71.69 ± 0.65
	No. of Solvent Molecules (5 Å)	
water	10.2 ± 1.6	2.6 ± 1.0
acetonitrile	0	4.8 ± 0.9
HB	183 ± 5.6	212 ± 6.0
SB	8.4 ± 1.7	13.0 ± 1.6

buried, accordingly inducing an increase in the hydrophobic SASA and a drop in the hydrophilic SASA.

It may be expected that solvent-buried residues would generally have the lower RMSF and solvent-exposed residues would have the higher RMSF. Figure 3 presents a comparison of the RMSF value with the SASA for every residue. As expected, high SASA values of residues almost correspond to high flexibility and low SASA almost correlate with low flexibility. Some groups[62,63] have reported the correlation between the solvent-accessible surfaces of residues and their flexibility, which are derived from statistical analysis on considerable proteins in terms of their structure and sequence information. Our MD simulations on the γ-chymotrypsin in the two media present a similar observation. As revealed above, the ACN system has a lower protein flexibility and smaller SASA than WAT. It seems that there is a positive correlation between the flexibility of protein and its total SASA, in agreement with the suggestion presented by Marsh[64] that proteins expose more solvent-accessible surface area and adopt a more extended conformation, and they are likely to be more flexible.

In fact, herein, we cannot directly quantify the thermostability of γ-chymotrypsin in acetonitrile media because thermodynamic quantities (for example, $\Delta G_{unfolding}$) cannot be calculated in the work. However, it was generally accepted that thermal stability of proteins can be a consequence of a reduced surface area,[65] which simultaneously reduces the unfavorable surface energy and increases the attractive interior packing interactions (for example, intraprotein hydrogen bonds and salt bridges, et al.). We also calculated intraprotein hydrogen bonds and salt bridges for the two media (see Table 2). We consider one hydrogen bond to be presented if both the distance between the hydrogen atom acceptor and hydrogen atom donor <3.5 and the angle between the hydrogen bond donor atom, hydrogen atom, and acceptor atom more than 120° criteria are satisfied simultaneously. A salt bridge is defined by a cutoff distance of 4.0 between the center of the oxygen atoms in an acidic residue and the center of the nitrogen atoms in a basic residue. As can be seen from Table 2, there are more hydrogen bonds and salt bridges in the ACN system than in the WAT system; thus, it is reasonable to assume that the decreased SASA and increased intraprotein hydrogen bonds and salt bridges should contribute to the higher thermal stability that enzymes usually present in organic solvents.[1−5] In addition, the acetonitrile induced an increase in

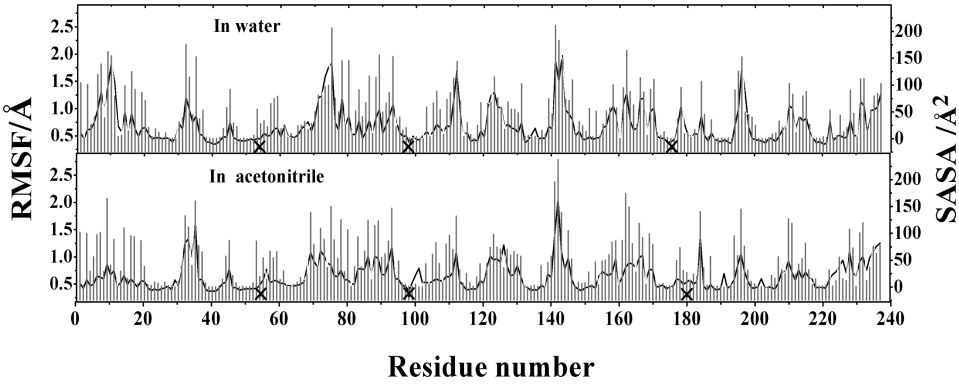

Figure 3. Average RMSF and SASA for each residue in the two media over the last 1 ns simulation. The black curve depicts the RMSF per residue, and the gray bar depicts the SASA per residue; x symbols denote catalytic residues.

dx.doi.org/10.1021/jp3002405 | J. Phys. Chem. B 2012, 116, 3292−3304

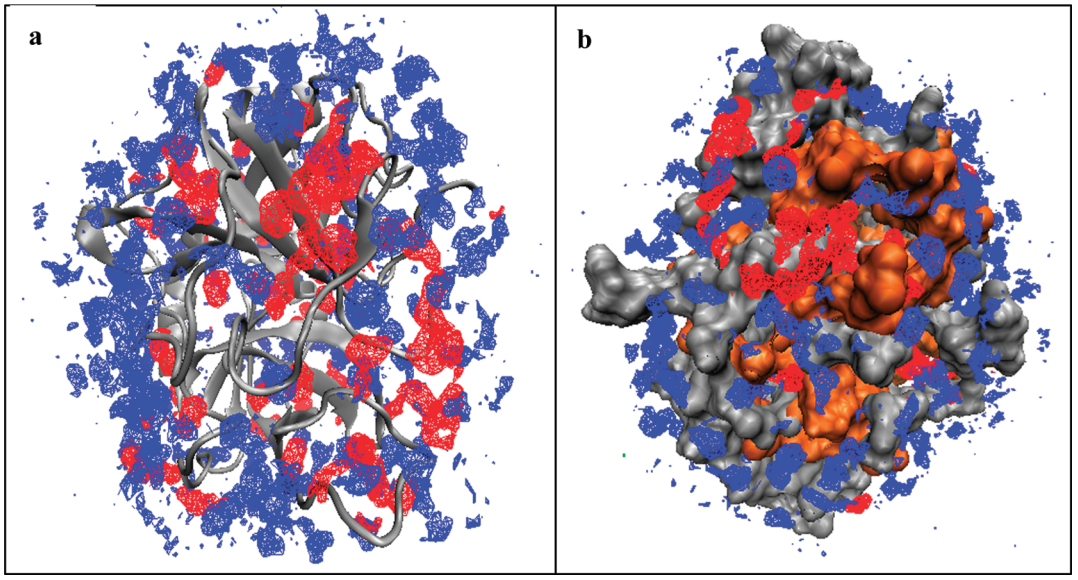

Figure 4. The spatial distribution of water and acetonitrile molecules around the protein, the protein corresponds to the average structure of γ-chymotrypsin over the last 1 ns equilibrium trajectory, the contours enclose regions with a probability density above 3 times the average density for water (red contour) and 13 times for acetonitrile (blue contour). The average structure of the enzyme was drawn according to the second structure (a) and the hydrophobic surface area (orange) and the hydrophilic surface area (silver) (b).

the intraprotein H-bonds that may be partly responsible for a drop in the flexibility of the protein in the organic solvent.

3.1.3. Solvent Distribution around Protein Surface and Penetration into the Active Site. Figure 4 presents the spatial probability density distribution of water (rendered as a red contour) and acetonitrile (rendered as a blue contour) around the protein in acetonitrile media, which were calculated by binning atom positions from rms coordinate fit frames over all protein atoms at 1 ps intervals into $(0.5\ \text{Å})^3$ grids over the last 1 ns trajectories. The number densities of the bulk water and acetonitrile are calculated to be 0.03344 and 0.0116, respectively. The contour level cutoff values in Figure 4 are 3 and 13 times average density of bulk water and acetonitrile solvents, respectively, which could provide a clear picture for the two solvent distributions around the protein. As shown in Figure 4a, the spatial contours enclosing high probability regions of finding the crystal waters are located mainly at the protein surface and a fraction in the protein interior. We also used smaller cutoff values (for example, 1−2 times average density of bulk water and 5−12 times average density of bulk acetonitrile) to observe the crystal water distribution (data are not shown). The results derived from different cutoff values are consistent with each other. It confirms that the crystal waters distribute mainly on the protein surface, and some reside inside the protein, not diffusing into the bulk acetonitrile media. Thus, these crystal waters, to some extent, could weaken the acetonitrile-induced variations on the structure of protein. In addition, Figure 4b further suggests that these crystal waters on the protein surface seem to be clustered mainly nearby the hydrophilic residues represented by the hydrophilic surface area.

As can be seen from Figure 4a, there are water and acetonitrile molecules penetrating into the protein interior. To gain further insight into the distribution of solvents in an active site, we calculated the average resident number of acetonitriles and waters in the active pocket, defined as the space within 5 Å centered at the atom OG@Ser195[15] (see Table 2). The data in Table 2 reveal that there are about 4.8 acetonitrile molecules and 2.6 water molecules residing in the pocket at any time during the last 1 ns trajectory for the ACN system, and there are 10.2 water molecules located in the active pocket for the WAT system, further confirming the penetration of the solvent molecule into the active site. Compared with the WAT system, many fewer water molecules residing in the pocket for the ACN system display a role of the acetonitrile molecule in preventing penetration of water molecules.

3.1.4. H-Bond Analysis in the Active Site. To gain insight into interactions between the solvent molecules in the active pocket and the active atoms of the protein, we carry out a detailed analysis of hydrogen bonding for the active site because H-bonding plays an important role in the catalytic activity of chymotrypsin.[22,23] It is noted that the criteria used for a hydrogen bond in the MD part are solely geometric.

In the crystal structure, two hydrogen bonds are presented between catalytic triads, as illustrated in Figure 1. Our simulations show that the H-bond between ND1@His57 and OD1@Asp102 exists in all simulations with a lifetime of 100% (see Table 3). The very stable H-bond between His57 and Asp102 was also observed for γ-chymotrypsin in nonpolar hexane media.[15] These observations indicate that the organic solvent, either polar or nonpolar organic solvents, hardly

Table 3. Average Distances of Hydrogen Bonds (in Å) and Their Percentage Occupation (%) and Standard Deviations over the Last 1-ns Simulation[a,b]

	NE2@His57-OG@Ser195		OD1@Asp102-ND1@His57	
system	X···Y	%		X···Y
WAT	3.342 ± 0.643	28	WAT	3.342 ± 0.643
ACN	5.225 ± 0.554	20	ACN	5.225 ± 0.554

[a]For the numbering scheme of the atoms and residues, see Figure 1. [b]OG@Ser195 denotes the OG atom of the Ser195 residue. NE2@His57 and ND1@His57 denote the NE2 and ND1 atoms of the His57 residue, respectively. OD1@Asp102 denotes the OD1 atom of the Asp102 residue.

dx.doi.org/10.1021/jp3002405 | J. Phys. Chem. B 2012, 116, 3292−3304

influence the H-bonding between ND1@His57 and OD1@Asp102, also implying strong H-bonding between the two residues. In contrast, significant effect of the solvent is observed for the H-bonding between the His57 residue and the Ser195. For the WAT and ACN systems, the hydrogen bond that is present in the crystal structure between the two residues is not as stable as that between the Asp102 residue and the His57. In most of the simulation time, the hydrogen bond between His57 and Ser195 is broken, and occasionally, hydrogen bonding is formed during 28% of the simulation times for the aqueous solution (averaged distance 3.342 Å) and 20% for a mixed solution (averaged distance 5.225 Å).

An occasional hydrogen bond was also found by Kato[29] for free chymotrypsin in aqueous solution. The observation suggests that the direct H-bond between His57 and Ser195 is broken in most simulation times. In addition, we analyze H-bonding between the two catalytic residues and solvent molecules penetrated into the active site (see Table 4). For the acetonitrile molecules, there is no H-bonding observed for them and the His57 residue, but they form an H-bond with the Ser195 residues over 18% simulation time. For the water molecules, it is observed that they form H-bonds with NE2@His57 over 186% and 126% simulation time in acetonitrile and aqueous solutions, respectively. The percentage occupation of H-bond over 100% is attributed to the fact that more than one water molecule simultaneously meets the criteria of H-bonding with the NE2@His57 atom within the calculation time. The water molecules form H-bonds with OG@Ser195 over 76% and 56% simulation times in the acetonitrile and aqueous solutions, respectively.

Table 4. The Percentage Occupation (%) of the Hydrogen Bond between the Catalytic Residue and the Solvent Molecule in Aqueous Solution (WAT) and Acetonitrile Media (ACN)[a,b]

	system	
heavy atoms of H-bond	WAT, %	ACN, %
OG@Ser195···O@H_2O	56	76
NE2@His57···O@H_2O	126	186
N@Gly193···O@H_2O	111	22
OG@Ser195···N@ACN	/	18
N@Gly193···N@ACN	/	57

[a]For the numbering scheme of atoms and residues, see Figure 1. [b]OG@Ser195 depicts OG atom of Ser195 residue. NE2@His57 depicts NE2 atom of His57 residue. N@Gly193 depicts nitrogen atom of Gly193 residue. N@ACN depicts nitrogen atom of the acetonitrile molecule. O@ H_2O depicts O atom of the water molecule. "/" denotes no interaction.

Further analysis revealed that the hydrogen linked to the OG@Ser195 atom, in more than half simulation time, is still interconnected to the oxygen atom of one nearby water molecule through H-bond contacts, and simultaneously, the water molecule also forms a hydrogen bond with the NE2@His57 atom. Figure 5a and b displays the distance between the OG@Ser195 atom and one water nearest to it and the distance between the same water molecule and the NE2@His57 atom as a function of time over the last 1 ns simulation in acetonitrile and aqueous solutions. It is clearly observed that there is always one water molecule in the space within 3 Å around OG@Ser195, implying possible H-bonding between the water molecule and the OG@Ser195 atom.

Furthermore, it is found from Figure 5a and b that the two curves are overlapped in most simulation time for the ACN system and occasionally overlapped for the WAT system. The overlapping suggests that the water molecule nearest to the OG@Ser195 atom should be located between the NE2@His57 atom and OG@Ser195, serving as a water bridge connecting the two atoms. Further H-bond analysis shows that the water molecule, as a bridge of the hydrogen bond, is not fixed on one water molecule. In the last 1 ns simulation time, it is observed that there are three water molecules for the ACN system and about 40 molecules for the WAT system, alternately penetrating into the active site and serving as a bridge of H-bond between His57 and Ser195. The observation derived from the H-bond analysis implies that the catalytic H-bond network is probably retained through one water bridge in the ACN system, suggesting the importance of the role of the essential water in maintaining the active structure of the protein.

3.2. QM Study on the Active Site. In this part, we further use the QM method to study the ACN and WAT systems to gain more insight into the effect of solvent on the active site. QM calculations involve only the reactive site, which consisted of a catalytic triad (viz., Asp102, His57, and Ser195), an oxyanion hole (viz., Gly193 and Ser195), and one hydrogen-bonding residue (viz., Ser214). The five residues were observed to play an important role in the function of chymotrypsin-like protease.[22,66] In the QM active model, these residues are truncated, and the cutoff fragments at the C atoms were substituted by H atoms. The truncated active site model was successfully used in the theoretical study on chymotrypsin in

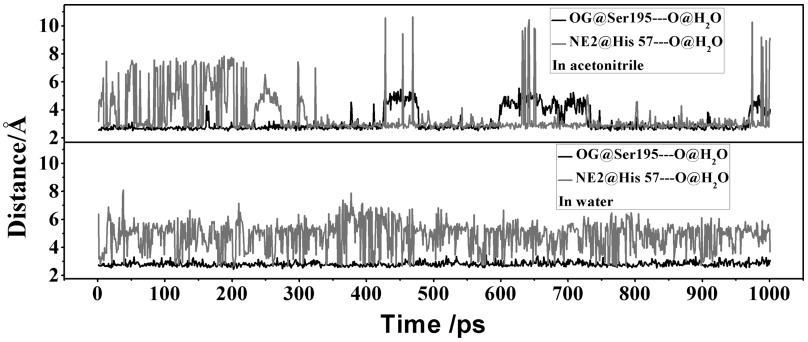

Figure 5. The time-dependent distances between the OG@Ser195 atom and the oxygen atom of the water molecule (O@H_2O) closest to it (labeled as OG@Ser195···O@H_2O) and between the same water molecule and the NE2@His57 atom (labeled as NE2@His57···O@H_2O) in acetonitrile (a) and water (b), derived from the last 1 ns simulation.

dx.doi.org/10.1021/jp3002405 | J. Phys. Chem. B 2012, 116, 3292−3304

aqueous media.[41,66−68] Different from the active model used in the previous studies, our QM models include two specific solvent molecules with an objective of gaining insight into the specific solvent effect on the active site. In addition, the PCM model is introduced in order to include the dielectric effects from the solvent and the protein surrounding, as mentioned in Computational Details.

Some theoretical research has indicated that protein dielectric constants, which are assigned in the range of 10−20,[68−70] could provide satisfactory results for p*K*a values of active residues. The MD simulation above showed that there are solvent molecules penetrating into the protein interior, and our QM models already include two specific solvent molecules. Thus, the dielectric constant in the PCM calculation is determined to be 15. In fact, the computational level could well reproduce some available experimental values, as demonstrated later. In the following discussions, we will focus on the effects of the specific solvent on properties associated with the H-bond network in the active site, which has been confirmed to be responsible for the activity of the enzyme.[22,23]

3.2.1. Setup of Initial Conformations of the Truncated Active Site Model. The initial conformation of the five active residues for the aqueous media was derived from the X-crystal structure. As revealed by the MD simulation in the aqueous solution, one water molecule may act as a bridge connecting His57 and Ser195, and one water molecule forms an H-bond with the N−H bond of Gly193 with a lifetime of 111% (see Table 4). It is accepted that the oxyanion hole is formed by the backbone NHs of Gly193 and Ser195[22] and these atoms form a pocket of positive charge that activates the carbonyl of the scissile peptide bond and stabilizes the tetrahedral intermediate. Thus, we considered the solvent molecule H-bonded with the N−H bond of the Gly193 residue in the truncated QM model. As a result, the QM active model in the aqueous solution (labeled as WAT) includes the two water molecules (viz., one water molecule as a bridge and one water molecule H-bonded with the Gly193 residue).

Owing to the unavailability of the X-crystal structure of chymotrypsin in the acetonitrile solvent, its active site model was constructed on the basis of the MD equilibration trajectory. We selected four snapshots (after 150, 300, 600, and 900 ps) from the last 1 ns trajectory in acetonitrile media. In addition, we also consider one average structure over 1000 snapshots taken at 1 ps intervals of the last 1 ns trajectory for the acetonitrile media, since the average structure may be more representative of what is observed experimentally by NMR or crystallography. Thus, in the QM study, the five conformations are selected as representative structures of the protein in acetonitrile media. The results from the five structures in acetonitrile media enable us to observe the effects of different conformations on the calculated properties.

Similarly, two solvent molecules are considered in the five structures, which form a H-bond with the O−H bond of the Ser195 and the N−H bond of the Gly193 residue, respectively, as revealed by the MD study above. The five truncated active site models derived from the four snapshots and the average structure in acetonitrile media are labeled as ACN150, ACN300, ACN600, ACN900, and ACN-avg, respectively. Figure 6 presents a superposition of the five models in acetonitrile media and one model in aqueous solution, where only the backbone of the residue is presented. It can be seen from Figure 6 that there are no significant displacements for the active residues in the six models, displaying the relative rigidity

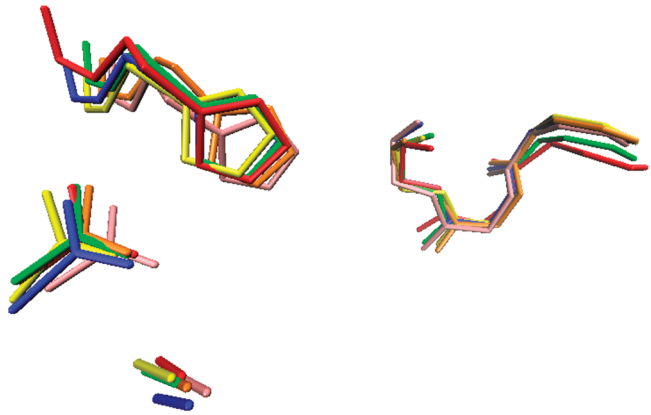

Figure 6. A superimposition of all truncated active site structures used in the QM study. Color code: orange, ACN150; yellow, ACN300; blue, ACN600; red, ACN900; green, ACN-avg; pink, WAT.

of the active site. Figure 7 further shows the structures of the six models optimized at the B3LYP/6-31+G** level of theory within the framework of the PCM model, along with the numbering scheme used in later discussions.

3.2.2. Geometric Analysis. As shown in Figure 7, the ACN300, ACN600, ACN900, and ACN-avg systems include one water molecule (labeled as H_2O1 in Figure 7) and one acetonitrile molecule (labeled as ACN2 in Figure 7). The four optimized structures well reproduce the water bridge and the H-bond between the acetonitrile molecule and the Gly193 residues, as revealed by the MD simulation above. Their stabilities are in the order of ACN-avg > ACN900 > ACN300 > ACN600, as indicated by their total calculated energies (data is not shown). However, the water bridge is not presented in the ACN150 model, where two acetonitrile molecules (labeled as ACN1 and ACN2 in the ACN150 system of Figure 7) are located in the active site and one of the two acetonitrile molecules instead of the water bridge presented in the other five models (viz., ACN300, ACN600, ACN900, ACN-avg, and WAT) inserts between the His57 and Ser195 residues.

Table 5 lists calculated intermolecular distances associated with possible H-bonding for the six models. As can be seen in Table 5, different conformations in the acetonitrile media lead to a slight difference in the calculated distances. For example, the calculated distance between the N2 atom (see Figure 7 for the numbering scheme of atoms) of the His57 residue (viz. N2@His57) and the oxygen atom of the Asp102 (viz. O@Asp102) changes by 0.075 Å with different snapshots, whereas the distance of the O@Asp102 and O@Ser214 changes by 0.011 Å.

For the Asp102 and His57 residues, the calculated distance of N1@His57···O@Asp102 in the WAT model is 2.759 Å, close to the experimental value of 2.70 Å reported by Harel.[71] It confirms that our computation level is reasonable. The distances of O@Asp102···N1@His57 and O@Asp102···H@His57 in the ACN150, ACN300, ACN900, and ACN-avg models are longer than that in WAT, as shown in Table 5. Although the distance of O@Asp102···N1@His57 in the ACN600 (2.748 Å) is shorter than that in the WAT system (2.759 Å), the distance of O@Asp102···H@His57 is still longer than that in the WAT model. Longer distances of O@Asp102···H@His57 for the five models in acetonitrile media imply that the penetration of the acetonitrile molecule into the

dx.doi.org/10.1021/jp3002405 | J. Phys. Chem. B 2012, 116, 3292−3304

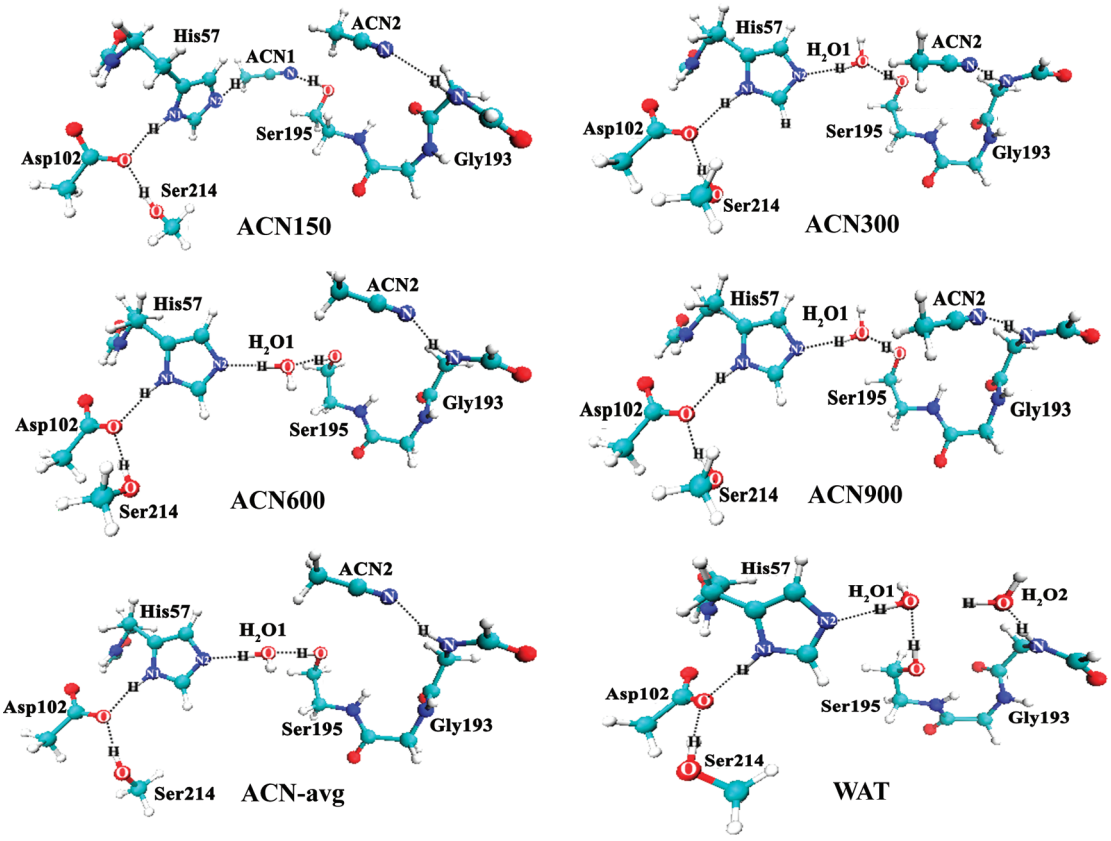

Figure 7. Structures of active site models in acetonitrile and aqueous solutions, optimized at the B3LYP/6-31+G** level of theory within the framework of the PCM model. The dotted lines denote H-bonds. Color code: white, hydrogen; red, oxygen; blue, nitrogen; cyan, carbon. For calculated intermolecular distances, see Table 5.

Table 5. Intermolecular Distances (X···Y) Associated with H-Bonding, Calculated at the B3LYP/6-31+G Level of Theory within the Framework of PCM Model[a]**

	distance (in Å)					
X···Y	ACN150	ACN300	ACN600	ACN900	ACN-avg	WAT
O@Asp102···N1@His57	2.823	2.787	2.748	2.769	2.761	2.759
O@Asp102···H1@His57	1.804	1.753	1.721	1.742	1.733	1.718
O@Asp102···O@Ser214	2.713	2.722	2.720	2.724	2.724	2.730
O@Asp102···H@Ser214	1.724	1.735	1.732	1.737	1.737	1.743
N2@His57···H@Sol[b]	2.343	1.783	1.745	1.748	1.740	1.686
X@sol···H@Ser195[c]	2.003	1.842	1.790	1.794	1.789	1.792
X@sol ···H@Gly193[d]	2.107	2.113	2.121	2.067	2.095	1.934

[a]For the numbering scheme of the atoms and molecules, see Figure 7. [b]N2@His57···X@sol denotes N2@His57···H@ACN1 in the ACN150 model, but it denotes N2@His57···H@H_2O1 in the other five models. [c]X@sol ···H@Ser195 denotes N@ACN1···H@Ser195 in the ACN150 model, but it denotes O@H_2O1···H@Ser195 in the other five models. [d]X@sol···H@Gly193 denotes O@H_2O2···H@Gly193 in the WAT model, but it denotes N@ACN2···H@Gly193 in the other five models.

active site would disfavor the interaction between the two residues.

As observed in Figure 7, there is one water molecule (denoted as H_2O1) inserted between the His57 and Ser195 residues in the ACN300, ACN600, ACN900, ACN-avg, and WAT systems. For the four models in acetonitrile media, the distances of H@H_2O1···N2@His57 are in the range of 1.740–1.783 Å, longer than that of the WAT system (1.686 Å). For the distances of O@H_2O1···H@Ser195, ACN600 and ACN-avg structures display slightly smaller values than the WAT, and an opposite trend is observed for the ACN300 and ACN900. For the ACN150 model, one acetonitrile molecule (denoted as ACN1) is located between the His57 and the Ser195 residues. The distance of H@ACN1···N2@His57 in the ACN150 model is calculated to be 2.343 Å, and that of N@ACN1···H@Ser195 is 2.003 Å, both longer than the corresponding distances between the water bridge and the two residues in the other five models. On the whole, it seems that the three molecules (viz., His57, the water bridge, and Ser195) in the WAT system are closer than those in acetonitrile media, implying a possibly weakened interaction among the three groups for the acetonitrile media.

For the Asp102 and Ser214, the distances of O@Asp102···O@Ser214 and O@Asp102···H@Ser214 are observed to be slightly longer in the WAT system than those in the acetonitrile media, as shown in Table 5. Toyokazu Ishida[29]

dx.doi.org/10.1021/jp3002405 | J. Phys. Chem. B 2012, 116, 3292–3304

reported that the distance between Asp102 and Ser214 becomes far in the process of the minimum energy reaction path of trypsin, derived from ab inito QM/MM calculations. In terms of the observation, it may be assumed that the penetration of acetonitrile solvent would disfavor the acylation reaction compared with that of the water molecule.

In addition, we also analyze the distance between the solvent molecule in the oxyanion hole (denoted as ACN2 or H_2O2) and the residue H-bonded to it. For the five models in acetonitrile media, the distances of H@Gly193···N@ACN2 are calculated to be 2.107−2.121 Å, all longer than that of H@Gly193···O@H_2O2 (1.934 Å) in the WAT model, implying a stronger interaction between the water molecule and the Gly193 residue than that between the acetonitrile molecule and the Gly193 residue.

On the whole, these important distance variations imply that the intermolecular interactions between these active residues would be weakened by the acetonitrile molecule.

3.2.3. ^1H NMR. Proton nuclear magnetic resonance spectroscopy (^1H NMR) is an attractive tool for studying hydrogen bonding in peptides and proteins, since the hydrogen nucleus is the most sensitive to the environment.[72−76] Herein, the ^1H NMR is calculated using the GIAO method at the B3LYP/6-311++G** level combining with the PCM model and listed in Table 6. The value of $\delta_{H@His57}$ in the WAT system is 15.6 ppm, which well reproduces the experiment value in aqueous solution (15.0 ppm) reported by Zhong,[77] providing support for the reliable computational model used in the work. The chemical shifts of H@His57 for the five models in acetonitrile media are in the range of 14.3−15.5 ppm, slightly smaller than that in the WAT model, suggesting that the penetration of the acetonitrile molecule slightly weakens the H-bonding of O@Asp102··· H@His57, in agreement with the observation derived from the geometric analysis above. Either for the systems in acetonitrile media or for the one in aqueous solution, the chemical shifts of H@His57 are larger than 14 ppm, suggesting that there should be strong H-bonding between the Asp102 residue and the His57, consistent with experimental observation.[78]

An inspection of Table 6 shows that the chemical shift of hydrogen nucleus of the solvent molecule as a bridge in the acetonitrile media (4.8−10.3 ppm) is smaller than that in the WAT (11.4 ppm) model, implying a weakness in the H-bond strength between the solvent molecule and the His57 residue caused by the acetonitrile molecule, especially for the ACN150 model. The chemical shift of H@Ser195 in the ACN150 system is much smaller (3.6 ppm) than the other four models in acetonitrile media and the WAT system. The chemical shifts of H@Ser195 in the ACN600, ACN900, and ACN-avg structures are slightly larger than that in the WAT system, and the one in the ACN300 displays a reverse trend. In addition, the chemical shifts of H@Ser214 change very little for the five models in the acetonitrile media (variation within 0.3 ppm) and slightly more than that in the WAT. Compared with the WAT system, a significant drop in the chemical shift of H@Gly193 is observed for the five models in the acetonitrile media, also implying weaker H-bonding between the acetonitrile molecule and the Gly193 residue. These observations are consistent with the results from the geometric analysis above and may provide theoretical information for spectroscopic study in the field. However, it is observed that the solvent-induced variation on the ^1H chemical shifts for the active residues is almost slight (except for the ACN150 system), suggesting that it may be difficult to determine the solvent-induced subtle structure variations in the interior of the protein by means of NMR experiments.

Table 6. ^1H Chemical Shifts (δ_H/ppm) Involved in Intermolecular H-Bonding, Calculated at the B3LYP/6-311++G Level of Theory within the Framework of the PCM Model, Based on the Geometry Optimized at the B3LYP/6-31+G** Level of Theory within the Framework of the PCM Model[a,b]**

system	$\delta_{H@His57}$	$\delta_{H@Ser214}$	$\delta_{H@Ser195}$	$\delta_{H@sol}$[d]	$\delta_{H@Gly193}$
ACN150	14.3	7.2	3.6	4.8	7.3
ACN300	15.0	7.0	5.5	9.6	7.5
ACN600	15.5	7.0	5.9	10.2	7.1
ACN900	15.2	6.9	6.0	10.1	7.5
ACN-avg	15.3	6.9	6.0	10.3	7.6
WAT	15.6 (15.0[c])	6.8	5.8	11.4	9.2

[a]For the numbering scheme of atoms and molecules, see Figure 7. [b]All the chemical shifts of the hydrogen nuclei are referenced to TMS. [c]The experimental value of the chemical shift of H@His57 for free chymotrypsin in aqueous solution.[77] [d]$\delta_{H@sol}$ represents $\delta_{H@ACN1}$ in the ACN150 model; it represents $\delta_{H@H_2O1}$ for the other five models.

3.2.4. NBO Analysis. To accurately determine the H-bond in the active site and explore the origin of the solvent effect on the H-bonding, we perform NBO analysis, which has been demonstrated to be quite successful in detecting and characterizing H-bonding.[76,79,80] Table 7 lists calculated second perturbation energies of intermolecular orbital interaction using the NBO method within the framework of the PCM model at the B3LYP/6-31+G** level of theory, on the basis of the optimized structures at the same level.

An inspection of Table 7 shows that there are interactions between thelone pair on the O@Asp102 ($n_{O(Asp102)}$) atom and the σ antibond orbital of N1−H bond of His57 ($\sigma^*_{N1-H@His57}$) in the six models, and their second-order perturbation energies $E^{(2)}$ associated with the interactions (viz., $E^{(2)}(n_{O(Asp102)} \rightarrow \sigma^*_{N1-H(His57)})$ are larger than 22 kcal·mol^{-1}, clearly confirming strong hydrogen bonding. Compared with the five models in the acetonitrile media, the $E^{(2)}(n_{O(Asp102)} \rightarrow \sigma^*_{N1-H1(His57)})$ value is larger in the WAT system. It confirms the suggestion derived from the geometric and ^1H NMR analysis that the acetonitrile molecule penetration into the active site would weaken the H-bonding between Asp102 and His57. As a result, the H-bond distance of O@Asp102···H@His57 becomes longer in the acetonitrile media, and the chemical shifts of H@His57 become smaller with respect to the WAT system, as observed above. Since the H-bonding between Asp102 and His57 plays an important role in stabilizing the intermediate formed in the rate-determining step of chymotrypsin,[72,81,82] it is reasonable to assume that the penetration of the acetonitrile molecule into the active site would disfavor the stabilization of the intermediate.

In addition, it is observed that there are interactions of $n_{N2(His57)} \rightarrow \sigma^*_{O-H(H_2O1)}$ and $n_{O(H_2O1)} \rightarrow \sigma^*_{O-H(Ser195)}$ for the four models in acetonitrile media (except for ACN150) and the WAT system, confirming indirect H-bonding between the Ser195 and His57 residues through one water bridge. Furthermore, the $E^{(2)}$ value associated with the $n_{N2(His57)} \rightarrow \sigma^*_{O-H(H_2O1)}$ interaction in the WAT system is 37.66 kcal·mol^{-1}, larger than those in the ACN300, ACN600, ACN900, and

dx.doi.org/10.1021/jp3002405 | J. Phys. Chem. B 2012, 116, 3292−3304

Table 7. The Second-Order Perturbation Energies ($E^{(2)}$/kcal·mol^{-1}) Associated with Lone Pair of Proton Acceptor and Proton Donating σ^* Orbitals, Calculated Using the NBO Method at the B3LYP/6-31+G** Level of Theory within the Framework of the PCM Model, on the Basis of the Optimized Structure at the Same Level[a]

	$E^{(2)}$ (kcal·mol^{-1})					
interactions	ACN150	ACN300	ACN600	ACN900	ACN-avg	WAT
$n_{O@Asp102}\rightarrow\sigma^*_{N1-H1@His57}$	22.46	28.33	31.28	29.20	29.99	32.09
$n_{O@Asp102}\rightarrow\sigma^*_{O-H@Ser214}$	26.45	24.42	24.22	23.99	23.88	23.34
$n_{N2@His57}\rightarrow\sigma^*_{X-H@sol}$[b]	5.42	27.22	31.03	30.36	31.64	37.66
$n_{X@sol}\rightarrow\sigma^*_{O-H@Ser195}$[c]	9.80	18.42	21.42	22.26	21.99	19.34
$n_{X@sol}\rightarrow\sigma^*_{N-H@Gly193}$[d]	9.13	9.28	8.57	11.83	9.6	14.93

[a]For the numbering scheme of the atoms and molecules, see Figure 7. [b]$\sigma^*_{X-H@sol}$ denotes $\sigma^*_{C-H@ACN1}$ in the ACN150 model; it denotes $\sigma^*_{O-H@H_2O1}$ in the other five models. [c]$n_{X@sol}$ denotes $n_{N@ACN1}$ in the ACN150 model; it denotes $n_{O@H_2O1}$ in the other five models. [d]$n_{X@sol}$ denotes $n_{O@H_2O2}$ in the WAT model; it denotes $n_{N@ACN2}$ in the other five models.

ACN-avg models (27.22−31.64 kcal·mol^{-1}), confirming weaker H-bonding between the His57 residue and the water bridge for the acetonitrile media. As a result, the distance of the N2@His57···H@H_2O1 in the aqueous solution is shorter than those in the acetonitrile media. The $E^{(2)}(n_{O(H_2O1)}\rightarrow\sigma^*_{O-H(Ser195)})$ values are slightly larger in the ACN300, ACN600, and ACN-avg structures than that in the WAT, and a reverse trend is observed for the ACN300.

Similarly, the distance of O@H_2O1···H@Ser195 almost displays a negative dependence on the $E^{(2)}(n_{O(H_2O1)}\rightarrow\sigma^*_{O-H(Ser195)})$ value in the ACN300, ACN600, ACN900, ACN-avg, and WAT models; namely, the larger the $E^{(2)}(n_{O(H_2O1)}\rightarrow\sigma^*_{O-H(Ser195)})$ value, the shorter the distance of O@ H_2O1···H@Ser195. Interestingly, it is observed that there are interactions of $n_{N2(His57)}\rightarrow\sigma^*_{C-H(ACN1)}$ and $n_{N(ACN1)}\rightarrow\sigma^*_{H-O(Ser195)}$, demonstrating the H-bonding between the acetonitrile molecule (viz., ACN1 in Figure 7) and the two residues. The MD results above also suggest that there is H-bonding between the acetonitrile molecule and the O−H bond of Ser195 over 18% of the simulation time, but the MD study could not observe the H-bonding between the N2@His57 and the acetonitrile molecule.

The NBO analysis further reveals that it is a weak hydrogen bond of the C−H···N type between the His57 residue and the acetonitrile molecule as a bridge, as indicated by the small $E^{(2)}(n_{N2(His57)}\rightarrow\sigma^*_{C-H(ACN1)})$ value (5.42 kcal·mol^{-1}). The result also displays a stronger ability of NBO analysis to characterize H-bonding than the semiempirical MD method. Compared with the interaction between the water bridge and the Ser195 residue, the value of $E^{(2)}(n_{N(ACN1)}\rightarrow\sigma^*_{H-O(Ser195)})$ is very small (9.80 kcal·mol^{-1}), also confirming that the H-bond between the acetonitrile molecule and the Ser195 residue is much weaker than that between the water bridge and the Ser195 residue. The observation indicates that the acetonitrile molecule could act as a H-bond bridge to indirectly retain the H-bonding between His57 and Ser195, but the H-bonding between the two residues and the acetonitrile bridge is very weak compared with that between the two residues and the water bridge. On the whole, the NBO analysis confirms that the penetration of the acetonitrile molecule into the active site weakens the H-bond strength of the catalytic H-bond network (viz., Asp102−His57−Ser195), as suggested by the geometric and NMR analysis above.

In addition, the $E^{(2)}(n_{O(Asp102)}\rightarrow\sigma^*_{O-H(Ser214)})$ value is slightly smaller in the WAT model than those of the five models in the acetonitrile media, confirming a slight weakness in the strength of the H-bond. Thus, a longer H-bond distance of O@Asp102···H@Ser214 and smaller chemical shifts of H@Ser214 are observed in the aqueous solution. Similarly, smaller $E^{(2)}(n_{N(ACN2)}\rightarrow\sigma^*_{N-H(Gly193)})$ values of the five models (8.57−11.83 kcal·mol^{-1}) in acetonitrile media than the $E^{(2)}(n_{O(H_2O2)}\rightarrow\sigma^*_{N-H(Gly193)})$ in the WAT system (14.93 kcal·mol^{-1}) confirms that the H-bonding between the acetonitrile molecule and the Gly193 residue is weaker than that between the water molecule and the residue.

3.2.5. pKa of His57 Prediction. The p*K*a (ionization constant) values of the active site residues in a protein could provide useful information for understanding its functionality, since many catalytic reactions are initiated by a proton transferring between the protein and the substrate. However, the p*K*a experimental determination on active site residues is difficult because of the complexity of the protein structure. Thus, an accurate evaluation of the p*K*a values for functionally important groups of a protein is a highly demanding issue in computational chemistry, thus attracting considerable interest from theory.[67,68,83]

To estimate the solvent effect on *K*a values of the active site residues, we herein calculated p*K*a values of the Nε atom of the active center His57 residues (viz., the N2@His57 atom in Figure 7) in the six models using the method described in Computational Details. In this method, the accurate calculations of the solvation free energy and the gas phase free energy are essential for estimation of pK_a. The solvation free energy of the proton ($\Delta G_s(H^+)$) was reported to be in the range of about −252.0 to −266.0 kcal·mol^{-1}.[84−88] Herein, the −264.61 kcal·mol^{-1} value of $\Delta G_s(H^+)$, derived from an exprimental thermodynamic cycle for acetic acid,[47] is considered to estimate the p*K*a of His57, since some computational results showed that the value is reasonable.[87,89] The −6.28 kcal·mol^{-1} value[90,91] is used for the absolute value of the gas phase free energy of the proton ($G_{gas}(H^+)$).

In addition, some research has already showed that the DFT method with inclusion of the PCM model could give a reasonable estimation of the two energies.[81−83,92−94] Thereby, in that part, the effect of the solvent molecule that penetrated into the active site on the p*K*a of His57 is estimated using the B3LYP/6-31G+(d,p) level of theory within the framework of the PCM model.

The calculated p*K*a values of His57 for the six models are listed in Table 8, along with the corresponding experimental pK_a values of chymotrypsin in aqueous solution.[95] It can be seen from Table 8 that the calculated p*K*a value of His57 in the WAT model is 7.8, very close to the experimental value of 7.5 of free chymotrypsin.[95] For the five models in acetonitrile

dx.doi.org/10.1021/jp3002405 | J. Phys. Chem. B 2012, 116, 3292−3304

Table 8. The pK_a Value of the His57 Residue and the Energy Barrier (ΔE, in kcal·mol^{-1}) of Proton Transfer from the Ser195 Residue to His57 in the Six Models

system	pK_a	ΔE
ACN150	7.9	39.57
ACN300	5.3	20.00
ACN600	6.7	17.98
ACN900	6.3	18.59
ACN-avg	7.3	17.98
WAT	7.8 (7.5[a])	15.41

[a]The experimental value of pK_a in aqueous solution.[95]

media, the p*K*a values are 7.9, 5.3, 6.7, 6.3, and 7.3 in the ACN150, ACN300, ACN600, ACN900, and ACN-avg structures, respectively, displaying significant effects of different conformations on the calculated property. For the four models in the acetonitrile media (excepting for ACN150), their p*K*a values (5.3−7.3) are smaller than that in the WAT model, although their H-bond catalytic network are also conserved by one crystal water molecule; however, the p*K*a value of the ACN150 (7.9) system is slightly larger than that of the WAT system (7.8). On the whole, the average p*K*a value (6.7) of the five models in acetonitrile media is still smaller than that of the WAT system (7.8), suggesting that the acetonitrile solvent may weaken the ability of N2@His57 to accept a proton.

As accepted, the most common mechanism of chymotrypsin-like serine proteases is the general base−acid catalytic reaction. In the catalytic mechanism, the proton on the hydroxyl of Ser195 is first transferred to N2@His57, which acts as a general base. Then the Ser195 attacks the carbonyl of the peptide substrate and forms a tetrahedral intermediate between it and the substrate, which is the rate-determining step. On the basis of the reaction mechanism, the weakened ability of His57 to accept a proton in acetonitrile media, which is suggested by the decreased p*K*a in the media, should disfavor the reaction step.

3.2.6. Energy Barriers of Proton Transfer from Ser195 to His57. As mentioned above, the proton transfer from the Ser195 residue to the His57 is revealed as the first step in the catalytic mechanism of chymotrypsin. Thus, we calculated the energy barrier of the proton transfer in the six models to more directly estimate the solvent effect on the reaction activity. The barriers were obtained by means of the difference between the ground and transition states. The transition and group states are optimized at the B3LYP/6-31+G(d,p) level of theory. Further single-point MP2/6-311++G(d,p)//B3LYP/6-31+G-(d,p) calculations within the framework of the PCM model are carried out to ensure reliable energy predictions. The calculated ΔE values are listed in Table 8. As shown in Table 8, the proton transfer barrier in the WAT system is 15.41 kcal·mol^{-1}, smaller than those of the five models in acetonitrile media, confirming that the acetonitrile solvent would disfavor the base−acid catalytic reaction initiated by the proton transfer. The highest barrier is observed for the ACN150 model (39.57 kcal·mol^{-1}). It is much larger than the other four models in acetonitrile media, in which one crystal water molecule acts as a H-bond bridge.

As revealed by the NBO analysis above, the H-bond strength of the catalytic H-bond network in the ACN150 model, which is indirectly retained through one acetonitrile molecule as a bridge, is very weak, as compared with the other models with one water molecule as a H-bond bridge. As a result, the highest energy barrier in the proton transfer reaction is observed for the ACN150 model. It suggests that the conformation of the ACN150 model with one acetonitrile molecule as a H-bond bridge should significantly disfavor the catalytic reaction, even if the p*K*a value of the His57 in the conformation is slightly larger than that in aqueous solution. The result further confirms the important role of crystal water in controlling the catalytic activity of the enzyme in acetonitrile media and suggests that one should be cautious if singly using the p*K*a parameter to predict the reaction activity.

4. CONCLUSIONS

Using combined MD simulation with QM calculation, we studied γ-chymotrypsin in aqueous solution and acetonitrile media with the inclusion of 151 crystal waters. The MD results indicate that the γ-chymotrypsin in acetonitrile solvent has larger mobility from the crystal structure and lower flexibility than that in aqueous solution. Although no unwinding or denaturation is observed for the enzyme in acetonitrile media within the scale of the simulation time, the acetronitrile solvent still causes reorientation of the hydrophobic and hydrophilic side chains. Accordingly, a decrease in the SASA and an increase in intraprotein H-bonds and salt bridges are observed, which may contribute to an increase in the thermal stability of the protein. The spatial density distribution of solvents indicates that the 151 crystal waters mainly cluster at the protein surface, and a fraction resides in the interior of the protein, not diffusing into the bulk acetonitrile media. Thereby, it is reasonable to assume that they to some extent weaken the effect of the acetonitrile solvent on the structure of the enzyme. Although it is observed that there are acetonitrile molecules penetrating into the active site, no significant variation is observed for the structure of the active residues, displaying relative rigidity and small mobility of the catalytic triad. In addition, the MD simulation shows that the direct hydrogen bond between the Ser195 and His57 residues is almost broken both in acetonitrile and aqueous solutions, but one water molecule probably acts as a H-bond bridge to link the two catalytic residues.

The QM results further confirm that the catalytic H-bond network of Asp102−His57−Ser195 in acetonitrile media could be indirectly retained through a water bridge in most cases. Interestingly, it is found that the acetontrile molecule could act as a very weak H-bond bridge to link the His57 and Ser195 residues. Although the five QM conformations in acetonitrile media, which are derived from the MD trajectory, lead to some changes in the calculated properties, their variation trends with respect to that in the aqueous solution are almost consistent. The trend indicates that the acetonitrile solvent penetrated into the active site would give rise to a weakness in the strength of the catalytic H-bond networks, as indicated by the calculated distances, the ^{1}H chemical shifts, and the second perturbation stabilization energies derived from NBO analysis. As a result, a drop in the p*K*a value of His57 and a rise in proton transfer barriers from Ser195 to His57 are observed for the system in acetonitrile media.

In summary, these observations derived from the MD and QM studies suggest that the drop in the enzymatic activity in acetonitrile media may be associated with the decreased flexibility, the weakened H-bond strength in active site, and the increased proton-transfer barrier. In addition, the crystal waters play an importance role in retaining the catalytic H-bond network and weakening the acetonitrile-induced variations on these properties above, which may contribute to the fact that

dx.doi.org/10.1021/jp3002405 | J. Phys. Chem. B 2012, 116, 3292−3304

the enzyme could retain catalytic activity in the microhydration acetonitrile media.

AUTHOR INFORMATION

Corresponding Author

*Fax: +86-028-85412907. E-mail: (X.P.) xmpuscu@scu.edu.cn; (M.L.) liml@scu.edu.cn.

Notes

The authors declare no competing financial interest.

ACKNOWLEDGMENTS

This project is supported by the National Science Foundation of China (Grant No. 20973115) and the International Science and Technology Cooperation Foundation of Sichuan province (Grant No. 2011H0003). The authors thank the referees for valuable comments on this manuscript.

REFERENCES

(1) Klibanov, A. M. *Nature* **2001**, *409*, 241−246.
(2) Halling, P. J. *Philos. Trans. R. Soc., B* **2004**, *359*, 1287−1297.
(3) Hudson, E. P.; Eppler, R. K.; Clark, D. S. *Curr. Opin. Biotechnol.* **2005**, *16*, 637−643.
(4) Mansfeld, J.; Ulbrich-Hofmann, R. *Biotechnol. Bioeng.* **2007**, *97*, 672−679.
(5) Serdakowski, A. L.; Dordick, J. S. *Trends Biotechnol.* **2007**, *26*, 48−54.
(6) Anthonsen, T.; Sjurnes, B. J. *Methods in Nonaqueous Enzymology*; Birkhauser-Verlag: Switzerland, Basel, 2000.
(7) Zaks, A.; Klibanov, A. M. *J. Biol. Chem.* **1988**, *263*, 3194−3201.
(8) Eppler, R. K.; Komor, R. S.; Huynh, J.; Dordick, J. S.; Reimer, J. A.; Clark, D. S. *Proc. Natl. Acad. Sci. U.S.A.* **2006**, *103*, 5706−5710.
(9) Clark, D. S. *Philos. Trans. R. Soc., B* **2004**, *359*, 1299−1307.
(10) Colombo, G.; Carrea, G. *J. Biotechnol.* **2002**, *96*, 23−33.
(11) Zheng, Q. C.; Li, Z. S.; Sun, M.; Zhang, Y.; Sun, C. C. *Biochem. Biophys. Res. Commun.* **2005**, *333*, 881−887.
(12) Hua, L.; Huang, X.; Zhou, R.; Berne, B. J. *J. Phys. Chem. B* **2006**, *110*, 3704−3711.
(13) Lin, Y. C.; Cao, Z. X.; Mo, Y. R. *J. Am. Chem. Soc.* **2006**, *128*, 10876−10884.
(14) Wu, R. B.; Xie, H. J.; Cao, Z. X.; Mo, Y. R. *J. Am. Chem. Soc.* **2008**, *130*, 7022−7031.
(15) Toba, S.; Hartsough, D. S.; Merz, K. M. Jr. *J. Am. Chem. Soc.* **1996**, *118*, 6490−6498.
(16) Soares, C. M.; Teixeira, V. H.; Baptista, A. M. *Biophys. J.* **2003**, *84*, 1628−1641.
(17) Micaelo, N. M.; Teixeira, V. H.; Baptista, A. M.; Soares, C. M. *Biophys. J.* **2005**, *89*, 999−1008.
(18) Díaz-Vergara, N.; Piñeiro, Á. *J. Phys. Chem. B* **2008**, *112*, 3529−3539.
(19) Micaelo, N. M.; Soares, C. M. *FEBS J.* **2007**, *274*, 2424−2436.
(20) Rezaei-Ghaleh, N.; Amininasab, M.; Nemat-Gorgani, M. *Biophys. J.* **2008**, *95*, 4139−4147.
(21) Li, C.; Tan, T. W.; Zhang, H. Y.; Feng, W. *J. Biol. Chem.* **2010**, *285*, 28434−28441.
(22) Hedstrom, L. *Chem. Rev.* **2002**, *102*, 4501−4524.
(23) Topf, M.; Richards, W. G. *J. Am. Chem. Soc.* **2004**, *126*, 14631−14641.
(24) Bjorup, P.; Wehtje, E.; Adlercreutz, P. *Biocatal. Biotransform.* **1996**, *13*, 189−200.
(25) Liu, P.; Tian, G.; Lo, W. H.; Lee, K. S.; Ye, Y. *Prep. Biochem. Biotechnol.* **2002**, *32*, 29−37.
(26) Noritomi, H.; Suzuki, K.; Kikuta, M.; Kato, S. *Biochem. Eng. J.* **2009**, *47*, 27−30.
(27) Shen, H. Y.; Tian, G. L.; Ye, Y. H. *J. Peptide Res.* **2004**, *65*, 143−148.
(28) Guzmán, F.; Barberis, S.; Illanes, A. *Electron. J. Biotechnol.* **2007**, *10*, 279−314.
(29) Ishida, T.; Kato, S. *J. Am. Chem. Soc.* **2003**, *125*, 12035−12048.
(30) Copeland, R. A. *Enzymes: A Practical Introduction to Structure, Mechanism, and Data Analysis*; 2nd ed.; John Wiley & Sons, Inc.: New York; 2000.
(31) Case, D. A.; Darden, T. A.; Cheatham, T. E., III; Simmerling, C. L.; Wang, J.; Duke, R. E.; Luo, R.; Crowley, M.; Walker, R. C.; Zhang, W.; Merz, K. M.; Wang, B.; Hayik, S.; Roitberg, A.; Seabra, G.; Kolossvary, I.; Wong, K. F.; Paesani, F.; Vanicek, J.; Wu, X.; Brozell, S. R.; Steinbrecher, T.; Gohlke, H.; Yang, L.; Tan, C.; Mongan, J.; Hornak, V.; Cui, G.; Mathews, D. H.; Seetin, M. G.; Sagui, C.; Babin, V.; Kollman, P. A. *Amber 10*, 10th ed.; University of California: San Francisco, 2008.
(32) Duan, Y.; Wu, C.; Chowdhury, S.; Lee, M. C.; Xiong, G.; Zhang, W.; Yang, R.; Cieplak, P.; Luo, R.; Lee, T.; Caldwell, J.; Wang, J.; Kollman, P. *J. Comput. Chem.* **2003**, *24*, 1999−2012.
(33) Jorgensen, W. L.; Chandrasekhar, J.; Madura, J. D.; Impey, R. W.; Klein, M. L. *J. Chem. Phys.* **1983**, *79*, 926−935.
(34) Wang, J.; Wolf, R. M.; Caldwell, J. W.; Kollman, P. A.; Case, D. A. *J. Comput. Chem.* **2004**, *25*, 1157−1174.
(35) Wang, J.; Wang, W.; Kollman, P. A.; Case, D. A. *J. Mol. Graph. Model.* **2006**, *25*, 247−260.
(36) Cohen, G. H.; Silverton, E. W.; Davies, D. R. *J. Mol. Biol.* **1981**, *148*, 449−479.
(37) Berendsen, H. J. C.; Postma, J. P. M; Van Gunsteren, W. F.; DiNola, A.; Haak, J. R. *J. Chem. Phys.* **1984**, *81*, 3684−3690.
(38) Ryckaert, J. P.; Ciccotti, G.; Berendsen, H. J. C. *J. Comput. Phys.* **1977**, *23*, 327−341.
(39) Darden, T.; York, D.; Pedersen, L. *J. Chem. Phys.* **1993**, *98*, 10089−10092.
(40) Essmann, U.; Perera, L.; Berkowitz, M. L.; Darden, T.; Lee, H.; Pedersen, L. G. *J. Chem. Phys.* **1995**, *103*, 8577−8593.
(41) Shokhen, M.; Albeck, A. *Proteins: Struct., Funct., Bioinf.* **2004**, *54*, 468−477.
(42) Nemukhin, A. V.; Grigorenko, B. L.; Rogov, A. V.; Topol, I. A.; Burt, S. K. *Theor. Chem. Acc.* **2004**, *111*, 36−48.
(43) Miertus, S.; Tomasi, J. *Chem. Phys.* **1982**, *65*, 239−245.
(44) Reed, A. E.; Curtiss, L. A.; Weinhold, F. *Chem. Rev.* **1988**, *88*, 899−926.
(45) Ditchfield, R. *Mol. Phys.* **1974**, *27*, 789−807.
(46) Wolinski, K.; Hilton, J. F.; Pulay, P. *J. Am. Chem. Soc.* **1990**, *112*, 8251−8260.
(47) Liptak, M. D.; Shields, G. C. *J. Am. Chem. Soc.* **2001**, *123*, 7314−7319.
(48) Magill, A. M.; Cavell, K. J.; Yates, B. F. *J. Am. Chem. Soc.* **2004**, *126*, 8717−8724.
(49) Frisch, M. J.; Trucks, H. B.; Schlegel, G. E.; Robb, M. A.; Cheeseman, J. R.; Scalmani, G.; Barone, V.; Mennucci, B.; Petersson, G. A.; Nakatsuji, H.; Caricato, M.; Li, X.; Hratchian, P. H.; Izmaylov, A. F.; Bloion, J.; Zheng, G.; Sonnenberg, J. L.; Hada, M.; Ehara, M.; Toyota, K.; Fukuda, R.; Hasegawa, J.; Ishida, M.; Nakajima, T.; Honda, Y.; Kitao, O.; Nakai, H.; Verven, T.; Montgomery, J. A., Jr.; Peralta, J. E.; Ogliaro, F.; Bearpark, M.; Heyd, J. J.; Brothers, E.; Kudin, K. N.; Staroverov, V. N.; Kobayashi, R.; Normand, J.; Raghavachari, K.; Rendell, A.; Burant, J. C.; Iyengar, S. S.; Tomasi, J.; Cossi, M.; Rega, N.; Millam, J. M.; Klene, M.; Knox, J. E.; Cross, J. B.; Bakken, V.; Adamo, C.; Jaramillo, J.; Gomperts, R.; Stratmann, R. E.; Yazyev, O.; Austin, A. J.; Cammi, R.; Pomelli, C.; Ochterski, J. W.; Martin, R. L.; Morokuma, K.; Zakrzewski, V. G.; Voth, G. A.; Salvador, P.; Dannenberg, J. J.; Dapprich, S.; Daniels, D. A.; Farkas, O.; Foresmman, J. B.; Ortiz, J. V.; Cioslowski, J.; Fox, D. J. *Gaussian 09*; 2nd ed.; Gaussian, Inc.: Wallingford, CT, 2009.
(50) Tejo, B. A.; Salleh, A. B.; Pleiss, J. *J. Mol. Model.* **2004**, *10*, 358−366.
(51) Bordes, F.; Barbe, S.; Escalier, P.; Mourey, L.; Andre, I.; Marty, A.; Tranier, S. *Biophys. J.* **2010**, *99*, 2225−2234.
(52) Yang, L.; Dordick, J. S.; Garde, S. *Biophys. J.* **2004**, *87*, 812−821.
(53) Yu, H. A.; Karplus, M.; Nakagawa, S.; Umeyama, H. *Proteins: Struct., Funct., Bioinf.* **1993**, *16*, 172−194.

(54) Reslow, M.; Adlercreutz, P.; Mattiasson, B. *Eur .J. Biochem.* **1988**, *177*, 313−318.
(55) Kise, H.; Fujimoto, K.; Noritomi, H. *J. Biotechnol.* **1988**, *8*, 279−290.
(56) Cerovsky, V.; Jakubke, H. D. *Enzyme Microb. Technol.* **1994**, *16*, 596−601.
(57) Simon, L. M.; Kotormán, M.; Garab, G.; Laczkó, I. *Biochem. Biophys. Res. Commun.* **2001**, *280*, 1367−1371.
(58) Kuszewski, J.; Gronenborn, A. M.; Clore, G. M. *J. Am. Chem. Soc.* **1999**, *121*, 2337−2338.
(59) Humphrey, W.; Dalke, A.; Schulten, K. *J. Mol. Graphics* **1996**, *14*, 33−38.
(60) Campbell, M. K. *Biochemistry*; 3rd ed.; Harcourt Brace College Publishers: Philadelphia, 1999.
(61) Darby, N. J.; Creighton, T. E. *Protein Structure*; Oxford University: Oxford, New York, 1993.
(62) Zhang, H.; Zhang, T.; Chen, K.; Shen, S.; Ruan, J.; Kurgan, L. *Proteins: Struct., Funct., Bioinf.* **2009**, *76*, 617−636.
(63) Gao, J.; Zhang, T.; Zhang, H.; Shen, S.; Ruan, J.; Kurgan, L. *Proteins: Struct., Funct., Bioinf.* **2010**, *78*, 2114−2130.
(64) Marsh, J. A.; Teichmann, S. A. *Structure* **2011**, *19*, 859−867.
(65) Arnold, F. H. *Curr. Opin. Biotechnol.* **1993**, *4*, 450−455.
(66) Shokhen, M.; Albeck, A. *Proteins: Struct., Funct., Bioinf.* **2000**, *40*, 154−167.
(67) Shokhen, M.; Khazanov, N.; Albeck, A. *Chembiochem* **2007**, *8*, 1416−1421.
(68) Shokhen, M.; Khazanov, N.; Albeck, A. *Proteins: Struct., Funct., Bioinf.* **2008**, *70*, 1578−1587.
(69) Demchuk, E.; Wade, R. C. *J. Phys. Chem.* **1996**, *100*, 17373−17387.
(70) Simonson, T.; Brooks, C. L., III. *J. Am. Chem. Soc.* **1996**, *118*, 8452−8458
(71) Harel, M.; Su, C. T.; Frolow, F.; Silman, I.; Sussman, J. L. *Biochemistry* **1991**, *30*, 5217−5225.
(72) Westler, W. M.; Weinhold, F.; Markley, J. L. *J. Am. Chem. Soc.* **2002**, *124*, 14373−14381.
(73) Parker, L. L.; Houkm, A. R.; Jensen, J. H. *J. Am. Chem. Soc.* **2006**, *128*, 9863−9872.
(74) Mennucci, B. *J. Am. Chem. Soc.* **2002**, *124*, 1506−1515.
(75) Bagno, A.; Rastrelli, F.; Saielli, G. *J. Org. Chem.* **2007**, *72*, 7373−7381.
(76) Chen, A. Q; Pu, X. M.; He, S. H.; Guo, Y. Z.; Wen, Z. N.; Li, M. L.; Wong, N. B.; Tian, A. M. *New J. Chem.* **2009**, *33*, 1709−1719.
(77) Zhong, S.; Haghjoo, K.; Kettner, C. *J. Am. Chem. Soc.* **1995**, *117*, 7048−7055.
(78) Robillard, G.; Shulman, R. G. *J. Mol. Biol.* **1972**, *71*, 507−511.
(79) Senthilkumar, L.; Ghanty, T. K.; Ghosh, S. K.; Kolandaivel, P. *J. Phys. Chem. A* **2006**, *110*, 12623−12628.
(80) Bleiholder, C.; Werz, D. B.; Köppel, H.; Gleiter, R. *J. Am. Chem. Soc.* **2006**, *128*, 2666−2674.
(81) Hudáky, P.; Perczel, A. *Proteins: Struct., Funct., Bioinf.* **2006**, *62*, 749−759.
(82) Radisky, E. S.; Lee, J. M.; Lu, C. J. K.; Koshland, D. E. Jr. *Proc. Natl. Acad. Sci. U.S.A.* **2006**, *103*, 6835−6840.
(83) De Abreu, H. A.; De Almeida, W. B.; Duarte, H. A. *Chem. Phys. Lett.* **2004**, *383*, 47−52.
(84) Conway, B. E. *Ionic Hydration in Chemistry and Biophysics*; Elsevier Scientific Pub. Co.: Amsterdam, New York, 1981.
(85) Marcus, Y. *Ion Solvation*; Wiley: New York, 1985.
(86) Florian, J.; Warshel, A. *J. Phys. Chem. B* **1997**, *101*, 5583−5595.
(87) Tawa, G. J.; Topol, I. A.; Burt, S. K.; Caldwell, R. A.; Rashin, A. A. *J. Chem. Phys.* **1998**, *109*, 4852−4863.
(88) Kelly, C. P.; Cramer, C. J.; Truhlar, D. G. *J. Phys. Chem. B* **2006**, *110*, 16066−16081.
(89) Zhan, C. G.; Dixon, D. A. *J. Phys. Chem. A* **2002**, *106*, 9737−9744.
(90) Magill, A. M.; Cavell, K. J.; Yates, B. F. *J. Am. Chem. Soc.* **2004**, *126*, 8717−8724.
(91) Gao, D.; Svoronos, P.; Wong, P. K.; Maddalena, D.; Hwang, J. *J. Phys. Chem. A* **2005**, *109*, 10776−10785.
(92) Fu, Y.; Liu, L.; Li, R. Q.; Liu, R.; Guo, Q. X. *J. Am. Chem. Soc.* **2004**, *126*, 814−822.
(93) Nielsen, P. A.; Jaroszewski, J. W.; Norrby, P. O.; Liljefors, T. *J. Am. Chem. Soc.* **2001**, *123*, 2003−2006.
(94) Gutowski, K. E.; Dixon, D. A. *J. Phys. Chem. A* **2006**, *110*, 8840−8856.
(95) Robillard, G. *J. Mol. Biol.* **1974**, *86*, 541−558.